Langmuir

ARTICLE

pubs.acs.org/Langmuir

Evaluation of Different Nonspecific Binding Blocking Agents Deposited Inside Poly(methyl methacrylate) Microfluidic Flow-Cells

Nam Cao Hoai Le,[*,†,∥] Vladimir Gubala,[†] Ram P. Gandhiraman,[†] Stephen Daniels,[†,‡] and David E. Williams[†,§]

[†]Biomedical Diagnostics Institute (BDI), Dublin City University, Dublin 9, Republic of Ireland

[‡]National Centre for Plasma Science and Technology (NCPST), Dublin City University, Dublin 9, Republic of Ireland

[§]MacDiarmid Institute for Advanced Materials and Nanotechnology, Department of Chemistry, University of Auckland, Auckland-1142, New Zealand

ABSTRACT: Poly(methyl methacrylate) (PMMA) flow-cells containing microwells were deposited with different nonspecific binding blocking agents, namely, bovine serum albumin (BSA), cationic lipid (DOTAP:DOPE) and diethylene glycol dimethyl ether (DEGDME). Water contact angle (WCA) and atomic force microscope (AFM) measurements were carried out to confirm the successful depositions of BSA, DOTAP, and DEGDME onto the PMMA surfaces. Fluorescent intensity measurements were performed to evaluate the degree of nonspecific adsorption of Cy5-labeled anti-IgG proteins onto plain and oxygen plasma-treated (PT) PMMA flow-cells as well as PMMA flow-cells deposited with different above-mentioned blocking agents. We then employed a label-free detection method called total internal reflection ellipsometry (TIRE) to evaluate the stability of the deposited blocking agents inside the PMMA flow-cells. It was found that, while DOTAP:DOPE was the best agent for blocking the nonspecific adsorption, it could be removed from the PMMA surfaces of the flow-cells upon rinsing with phosphate buffered saline (PBS) and later deposited back onto the Au-coated glass sensing substrate of the TIRE. The removal of the blocking agents from PMMA surfaces and their deposition onto the sensing substrate were further manifested by measuring the kinetics and the amount of adsorbed anti-α-hCG proteins. Overall, the dry DEGDME coating by plasma-enhanced chemical vapor deposition (PECVD) showed very good blocking and excellent stability for subsequent assay inside the microwells. Our results could be useful when one considers what blocking agents should be used for PMMA-based microfluidic immunosensor or biosensor devices by looking at both the blocking efficiency and the stability of the blocking agent.

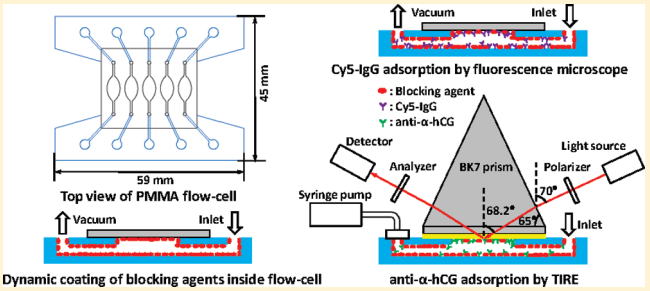

1. INTRODUCTION

Micro-total analysis systems (μ-TASs), also called "lab-on-a-chip", can acquire, separate, and analyze a variety of samples, and the microsizing and integration of these functions promises enormous medical and economic benefits.[1−4] Their small size, decreased analytical time, and tiny sample consumption help to improve bioassay performance. Poly(methyl methacrylate) (PMMA) is an excellent polymer material to be employed in the manufacturing of low-cost μ-TAS devices since it possesses excellent optical, thermal, chemical, and biocompatibility properties. However, during the functioning of PMMA-based μ-TAS devices, cells, proteins, or oligonucleotides in solution are exposed to a large hydrophobic PMMA surface area. Accordingly, one of the biggest problems with PMMA-based μ-TAS devices is that they could nonspecifically absorb a large amount of analytes.[5−8] For example, in PMMA-based electrophoresis separation devices, the nonspecific adsorption could result in band broadening, poor resolution, analytical irreproducibility and low separation efficiency. These effects are believed to be largely caused by nonuniform electroosmotic flow due to the inhomogeneous zeta potential along the separation length of the PMMA devices fouled with nonspecifically bound proteins and DNA.[6−9] Furthermore, when highly concentrated samples are used in these separation devices, this nonspecific absorption may cause clogging of the devices.[5] On the other hand, when low concentrations of samples are used in PMMA-based immunoassay and biosensor devices, the sample loss caused by nonspecific adsorption could mean a significant diminution in analyte concentration present at the functional (i.e., sensing or detection) components of the devices.[5−7]

Numerous methods have been proposed to modify the surface of PMMA to reduce the nonspecific adsorption of biomolecules.[8] The reported modification methods could be broadly categorized into dynamic coating and permanent modification by means of chemical reactions. Lin et al.[9] used a dynamic coating technique to deposit PMMA channels with poly(ethyleneoxide) (PEO). A hybrid dynamic coating of *n*-dodecyl β-D-maltoside (DDM) and methylcellulose (MC) has been developed by Dang et al.[10] to suppress analyte adsorption inside a PMMA microchannel. Similarly, Mohamadi et al.[11] reported a dynamic coating of MC and a nonionic detergent (polysorbate 20) onto a PMMA channel also for

Received: March 28, 2011
Revised: June 3, 2011
Published: June 07, 2011

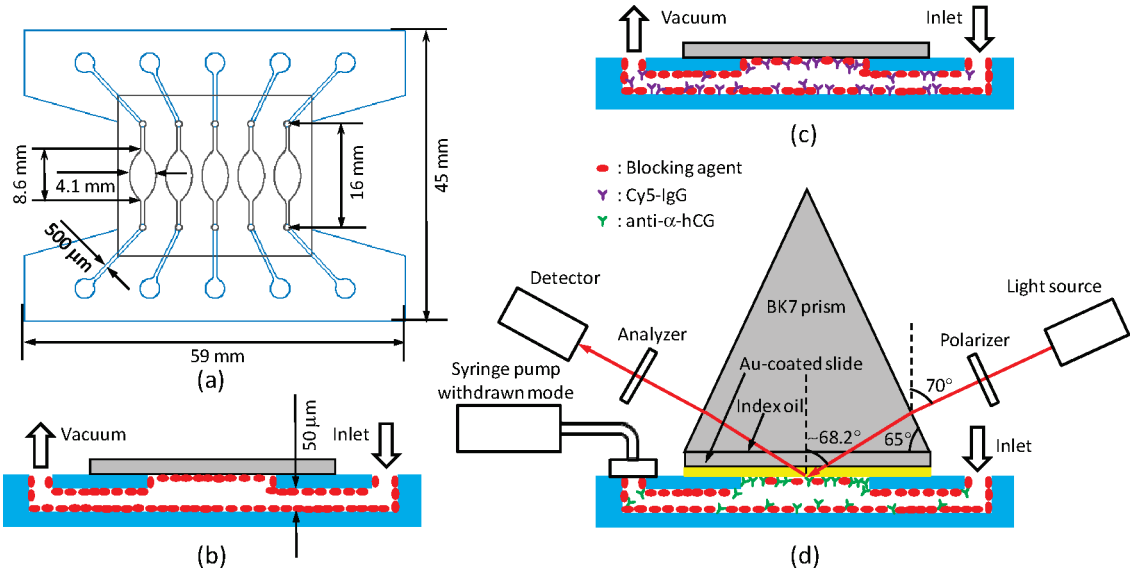

Figure 1. (a) Top view of the PMMA flow-cell with five microwells. (b) Cross-sectional view of one microwell of the PMMA flow-cell closed with a COP lid during the deposition of BSA, DOTAP:DOPE, or DEGDME by wet chemistry. (c) Cross-sectional view of the same microwell in panel b during the adsorption of Cy5-labeled anti-IgG for fluorescent measurements. (d) TIRE experimental setup on a spectroscopic ellipsometer with a PMMA microwell, a Au-coated glass slide, a BK7 prism, and a syringe pump.

suppressing the protein adsorption. On the other hand, permanent modification of the PMMA surface by surface chemistry, mostly with PEG derivatives, has also been used to reduce the nonspecific adsorption of analyte onto the PMMA surfaces. Lai et al.[12] employed a UV-initiated polymerization technique to immobilize poly(hydroxyethyl methacrylate-*co*-ethylene glycol dimethacrylate) on the internal walls of the channels forming a monolithic stationary gel for an acrylamide separation of DNA. An atom-transfer radical polymerization method was developed by Bi et al.[7] to form poly(ethylene glycol dimethacrylate-*co*-methylether methacrylate) copolymer on the surface of PMMA chips for increasing the hydrophilicity and electrophoretic separation of proteins. A similar chemistry has been adopted by Liu et al.[13] to graft poly(ethylene glycol) (PEG) on the PMMA surface after the deposition of 2-bromoisobutyryl bromide. The majority of these PMMA devices and their associated nonspecific binding coatings are designed for electrophoresis and separation. Although these above-mentioned modification methods have been successful in reducing the nonspecific adsorption of biomolecules onto the PMMA surfaces, to the best of our knowledge there has been no study on the stability of such coatings in contact with buffers and the effect on subsequent assays performed on PMMA devices integrated with a sensing element.

This paper reports a comprehensive comparison among different coatings for reducing nonspecific adsorption on the PMMA surface and the effect of the stability of the coatings with respect to assays performed on a gold sensing element integrated inside a PMMA flow-cell. To this end, the PMMA surface of the flow-cells has been modified by dynamic coating with bovine serum albumin (BSA) and cationic lipid DOTAP:DOPE (used as a 1:1 mixture of 1,2-di-(9Z-octadecenoyl)-3-trimethylammonium-propane (chloride salt) (DOTAP) and 1,2-dioleoyl-*sn*-glycero-3-phosphoethanolamine (DOPE)), by wet chemical deposition of diethylene glycol dimethyl ether (DEGDME) to form a PEG-type film and by plasma-enhanced chemical vapor deposition (PECVD) of dry DEGDME, again to form a polymeric ethyleneglycol-ether-type film. Water contact angle (WCA) and atomic force microscopy (AFM) were employed to confirm the successful surface modifications of the PMMA surface. Fluorescent intensity was measured inside the microwells of the PMMA flow-cells to evaluate the effectiveness of each coating against the nonspecific adsorption of Cy5-labeled anti-IgG. Finally, total internal reflection ellipsometry (TIRE)[14−21] with spectra and kinetic data of adsorption of anti-α-human chorionic gonadotropin (anti-α-hCG) was used to evaluate the stability of the coatings under buffer rinsing. Our results and methodology could be useful for choosing a blocking agent, its deposition, and characteristics for suppression of nonspecific binding of biomolecules on a PMMA surface, as part of the design and development of PMMA-based microfluidic immunosensors and biosensors.[22−26] In that regard, a good coating needs not only to effectively suppress the nonspecific adsorption of biomolecules, but also must show stability under prolonged rinsing and immersing with buffer, and in particular should not desorb from the PMMA and transfer onto the sensing element.

2. EXPERIMENTAL SECTION

2.1. Materials. Cyclo-olefin polymer (COP) slides (Zeonor 1060R) (25 mm ×75 mm, 1 mm thick) were supplied by Åmic AB (Uppsala, Sweden). PMMA sheets (0.25 mm thick, size 600 mm ×600 mm, impact modified) were supplied by Goodfellow Cambridge Limited (Huntingdon, England). Double-coated pressure-sensitive adhesive (PSA) tapes (50 μm thick, AR8890) were purchased from Adhesives Research Ireland, Ltd. (Limerick, Ireland). Gold-coated standard glass slides (Ti/Au = 2 nm/48 nm, 26 mm ×76 mm, 1 mm thick) were purchased from Phasis Sarl (Geneva, Switzerland). Transfection reagent I containing DOTAP:DOPE (1:1 w/w) was obtained from Avanti Polar Lipids, Inc. (Alabaster, AL, U.S.A.). Phosphate buffered saline (PBS, pH 7.4, 0.01 M), BSA (98%), tetraethyl orthosilicate (TEOS, 99.999%, $Si(OC_2H_5)_4$, and DEGDME ($CH_3O(CH_2CH_2O)_2CH_3$) were all purchased from Sigma Aldrich (Dublin, Ireland). All chemicals were used as received without further purification. The Cy5-labeled antihuman IgG was purchased from Molecular Probes (Eugene, OR). The anti-α-hCG

dx.doi.org/10.1021/la2011502 |*Langmuir* 2011, 27, 9043–9051

(clone 3299:4) was kindly donated by Inverness Medical Innovations (Bedford, U.K.).

2.2. Deposition of Blocking Agents into PMMA Microfluidic Flow-Cells. The five-microwell flow-cell, containing four layers, was fabricated in PMMA and PSA using a CO_2 ablation laser machining system (Figure 1a). The fabrication method of the PMMA flow-cell has been reported elsewhere.[21] For deposition of BSA and DOTAP:DOPE, a standard COP slide was glued to the top PSA layer of a PMMA flow-cell to form a closed channel, as shown in Figure 1b. Fifty microliters of BSA 1 wt % in PBS and 50 μL of 50 mM DOTAP:DOPE in deionized (DI) water was deposited at the two inlets of two nearby microwells of a half of the flow-cell. A vacuum was applied at the outlets of the two microwells to withdraw the liquid into the microwells. The solutions of BSA and DOTAP:DOPE were allowed to adsorb to the PMMA microwell for 60 min, rinsed by 50 μL of PBS twice, and dried with nitrogen.[27−30] Another flow-cell was oxygen plasma treated for 5 min and closed with a COP slide before 50 μL of 50 mM DEGDME was applied in the same fashion as that for BSA and DOTAP:DOPE. The DEGDME solution was also allowed to react for 60 min before being rinsed by 50 μL PBS twice and dried with nitrogen. For deposition of dry DEGDME by PECVD, the open PMMA flow-cell was subjected to plasma cleaning and activation in an argon plus oxygen mixed plasma, with a flow rate of 100 standard cubic centimeters per minute (sccm) of argon and oxygen, for 1 min at 100 W. This plasma-activated PMMA surface is referred to in the following sections as plasma-treated (PT) PMMA. Then the DEGDME deposition was carried out by sequential deposition of TEOS and DEGDME by low-pressure PECVD.[31−33] The flows of TEOS and DEGDME were controlled using needle valves, and the deposition was carried out in an argon plasma. The details about the PECVD chamber can be found elsewhere.[34] All the depositions mentioned above were repeated on flat PMMA sheets for WCA and AFM measurements.

2.3. Water Contact Angle. The wettability of different deposited films on PMMA sheets were analyzed by measuring the WCA of the surfaces using the First Ten Angstroms FTA200 (Portsmouth, VA) contact angle analyzer. In order to guarantee the flatness of the PMMA sheets, they were glued to PSA layers on top of glass slides before measurements. High-purity HPLC-grade water (Sigma Aldrich, Dublin, Ireland) was used for the measurement. The WCA of each of the deposited films was measured three times at three locations on the PMMA sheets.

2.4. Atomic Force Microscopy. AFM was used to compare the topographical surface created by the various surface modification processes. Similar to WCA measurements, the PMMA sheets were also glued to PSA layers on top of glass slides before AFM measurements. A Digital Instruments BioScope II (Veeco Instruments, Inc., Plainview, NY, U.S.A.) operating in contact mode under ambient conditions was used. Images were acquired with a silicon tip mounted on a silicon nitride cantilever (Veeco Probes, Camarillo, CA, U.S.A.) with a spring constant of 0.06 N/m operating at a resonant frequency of 12−24 kHz and at a scan rate of 0.25 Hz. Coated and uncoated PMMA surfaces were analyzed over three 5 μm × 5 μm areas at a resolution of 256 × 256 pixels, and images were produced using Research NanoScope 7.30 software (Veeco Instruments, Inc.). Zero-order plane fitting was used to remove the image bow that can result from the scanner moving out of plane with the sample.

2.5. Fluorescent Microscopy. After the deposition of the BSA, DOPTAP:DOPE, and wet DEGDME blocking agents, the COP lids of the PMMA flow-cells were replaced with new COP lids since the PSA layer still maintain its adherence toward COP several times. For plain and PT PMMA and dry DEGDME-coated PMMA, the COP lids were applied to the PSA layer for the first time to form a closed channel. Thirty microliters of 25 μg/mL of Cy5-anti-IgG in PBS (pH 7.4) was applied in each microwell of the PMMA flow-cell using a vacuum and allowed to react for 1 h before being rinsed by PBS and dried with nitrogen. The COP lids were removed from the PMMA flow-cell before observation with fluorescent microscope. An inverted fluorescence microscope (IX81, Olympus Co., Japan) equipped with an EMCCD camera (DV887-BI, Andor Technology, UK) cooled to 0 °C and an MT20 fluorescence illumination unit fitted with a 150 W xenon lamp was used in combination with a MCy5 filter set to image the fluorescence of the Cy5-labeled anti-IgG proteins. The fluorescence inside the microwells of the flow-cell was obtained using a UPlanSApo objective lens, 4×, NA 0.16 (Olympus Co., Japan). The fluorescent images were acquired using the Cell^R software (Olympus Soft Imaging Solutions GmbH, Germany). All fluorescent images were acquired using the same set of parameters (exposure time of 330 ms, lamp power of 77.9%, EM gain of 94, resolution of 512 × 512 pixels (2.048 × 2.048 mm^2)). The fluorescence intensity was quantified using Wasabi software (version 1.50, Hamamatsu Photonics Germany GmbH, Germany) in a rectangular area of 500 μm × 1000 μm in each image captured.

2.6. Total Internal Reflection Ellipsometry. The TIRE experimental setup was based on the UVISEL spectroscopic ellipsometer (Jobin Yvon Horiba, France) (Figure 1d).[21] The Au-coated glass sensing substrate was first glued to the PMMA flow-cell by adhesion of the PSA reaction microwell layer. A BK7 prism was placed on top of the sensing substrate with intermediate refractive index matching oil and secured by tapes (Figure 1d). A syringe pump (Harvard Apparatus, Boston, U.S.A.) was connected to the outlet of one microwell of the flow-cell through polymer tubing and a polydimethylsiloxane (PDMS) connector for performing one assay at a time. Two modes of measurements were carried out with TIRE: kinetic and spectral measurement. In both modes, the Ψ and Δ values defined by the ratio ρ of the reflection coefficients R_p and R_s for components of light polarized parallel (p) and perpendicular (s) to the plane of incidence following the ellipsometry equation were measured.[15]

A droplet of PBS buffer was injected at the inlet of the microwell and was withdrawn into the microwell by the syringe pump operating under the withdrawn mode. New droplets of PBS buffers were injected at the same inlet when the previous droplet was nearly emptied. The flow rate of the syringe pump was set at 5 μL/min for a period of 15 min. Afterward, the first set of Ψ and Δ spectra were recorded at an angle of incidence of 70° with wavelengths ranging from 400 to 850 nm. The integration time was 200 ms, and the spectral resolution was 2 nm. After the first Ψ and Δ spectra were recorded, the kinetic measurement mode was turned on at a fixed wavelength, i.e., around 3-nm shift from the surface plasmon resonance (SPR) wavelength obtained from the first Ψ spectrum.[17,18] The integration time and interval in kinetic mode were both set at 100 ms, respectively. The syringe pump was operated again at a flow rate of 5 μL/min after the inlet of the microwell was deposited with a droplet of anti-α-hCG 50 μg/mL in PBS buffer (pH 7.4). New droplets were injected for a total period of the kinetic measurement of 60 min. The kinetic mode was turned off and the spectral mode was restarted to measure the second Ψ and Δ spectra corresponding to the adsorption of anti-α-hCG to the Au-coated glass surface. Although the flow-cell contains five microwells, only one assay was performed at a time on one microwell to prevent any possible shifting of the light rays in the optical setup. PsiDelta 2 software (Jobin Yvon Horiba, France) was used for fitting the data from the measured Ψ and Δ spectra from TIRE. A four-layer model similar to the model used in refs 16, 18, and 21 was used in the fitting to estimate the thickness of the organic layer first deposited onto the Au surface and then the thickness of anti-α-hCG.

3. RESULTS AND DISCUSSION

3.1. Deposition of Blocking Agents onto PMMA Surfaces. The successful depositions of the blocking agents were confirmed by comparison of the wettability and the morphology of the PMMA sheets deposited with BSA, DOTAP:DOPE, wet DEGDME, and dry DEGDME and with those of oxygen PT and

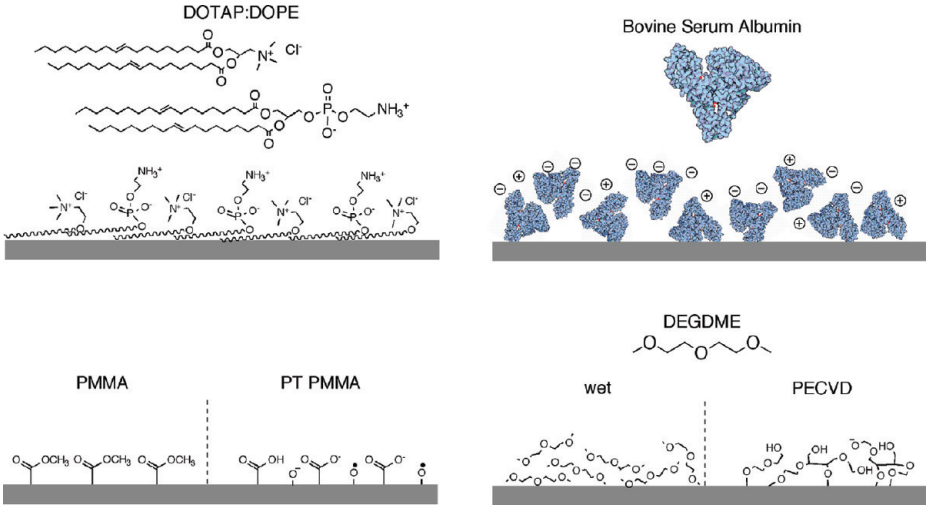

Figure 2. A schematic illustrating the nature of the chemical groups present on the PMMA surface (only the top layers are shown) after treating the pristine PMMA with DOTAP:DOPE mixture, BSA, plasma (PT), and DEGDME (wet deposition and PECVD).

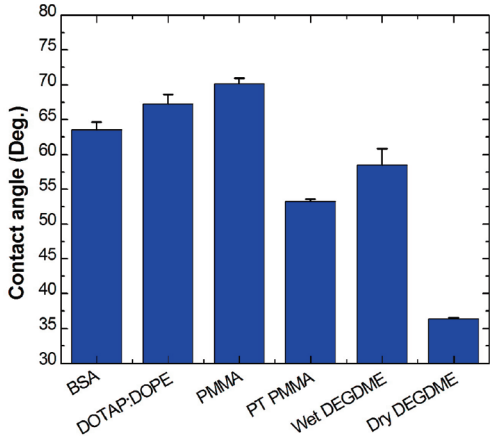

Figure 3. WCAs measured on PMMA sheets coated with different blocking agents. As a comparison, the WCA of the plain PMMA and PT PMMA are also shown. While coatings of BSA and DOTAP:DOPE result in only small changes in WCA, PT and wet DEGDME coating result in significant change in the contact angle. The dry DEGDME coating gave the highest reduction in WCA. Note that the dry DEGDME coating is different from the wet DEGDME coating: the underlying TEOS matrix might have contributed to this difference.

plain PMMA sheets (Figure 2). The differences in contact angles are attributed to the nature of the surface-exposed chemical groups after the depositions. The contact angle 70° of plain PMMA was slightly reduced after it was deposited with BSA or DOTAP:DOPE (Figure 3). We reason that the deposition mechanism for DOTAP:DOPE involves self-assembly driven by favorable electrostatic interactions between the negatively charged phosphate of DOPE and positively charged trimethyl-amine of DOTAP followed by adsorption of the hydrophobic tail of both compounds onto the PMMA surface thus exposing the ethanol-amine "head" as illustrated in Figure 2. BSA on the other hand might adsorb in layers, in which the BSA molecules at the bottom change their conformation, exposing some of the hydrophobic amino acids to make good contact with the PMMA. Another layer(s) of BSA might then adsorb on it, mainly through protein−protein interactions. The PMMA WCA dropped significantly after the deposition of wet and dry DEGDME as well as after plasma treatment. The largest drop is seen after the dry DEGDME deposition, which brings the contact angle down to 35° (Figure 3). It should be noted that the composition of the dry DEGDME is different from that of the wet DEGDME. The wet DEGDME film contains unfragmented DEGDME molecules, whereas the dry DEGDME film is composed of an underlying TEOS layer and cross-linked DEGDME molecules. The very low WCA of the dry DEGDME PMMA sheet is suggesting that TEOS might be inserted into the DEGDME layer and an effective plasma polymerization had taken place. In general, plasma deposition leads to fragmentation of the DEGDME precursor, thus some charged residues (with $-O^-$ group) and hydroxyl groups are likely to be formed. The hydrophilic nature of this surface is also explained by the presence of the silanols (from TEOS), although we can only speculate whether such groups are available on the top surface or are embedded in the bulk layer. Similar fragmentation effects could also be seen on the PT PMMA slide. Presumably, some of the methyl esters are oxidized into carboxylic acids. Other highly reactive species might appear too, such as oxygen radicals and anions. However, they are highly reactive and unstable over long periods of time. The morphologies of PMMA sheets deposited with different blocking agents are shown in Figure 4. The plain PMMA surface was not smooth, having scattered craters throughout (rms = 4.06 ± 0.50 nm) (Figure 4c). However, after BSA deposition, the craters on the surface were filled with BSA, and the surface became uneven (rms = 9.62 ± 2.58 nm) (Figure 4a). The coating of DOTAP:DOPE on PMMA made the surface become slightly more even thanks to the filling of DOTAP:DOPE into the craters (rms = 4.49 ± 0.09 nm) (Figure 4b). After deposition with wet DEGDME, the surface became more wavy and uneven (rms = 16.63 ± 3.17 nm) as seen in the case of BSA deposition (Figure 4e). However, of all the deposition methods, the sequential deposition of TEOS and DEGDME on the PT PMMA resulted in the roughest surface (rms = 21.1 ± 9.46 nm) as seen in Figure 4f. Interestingly, the dry DEGDME film was the only film the roughness of which further increased upon contact with water (data not shown) due to its swelling properties. This surface appears to become very well hydrated, with a structure perhaps resembling that of a hydrogel.

dx.doi.org/10.1021/la2011502 |*Langmuir* 2011, 27, 9043–9051

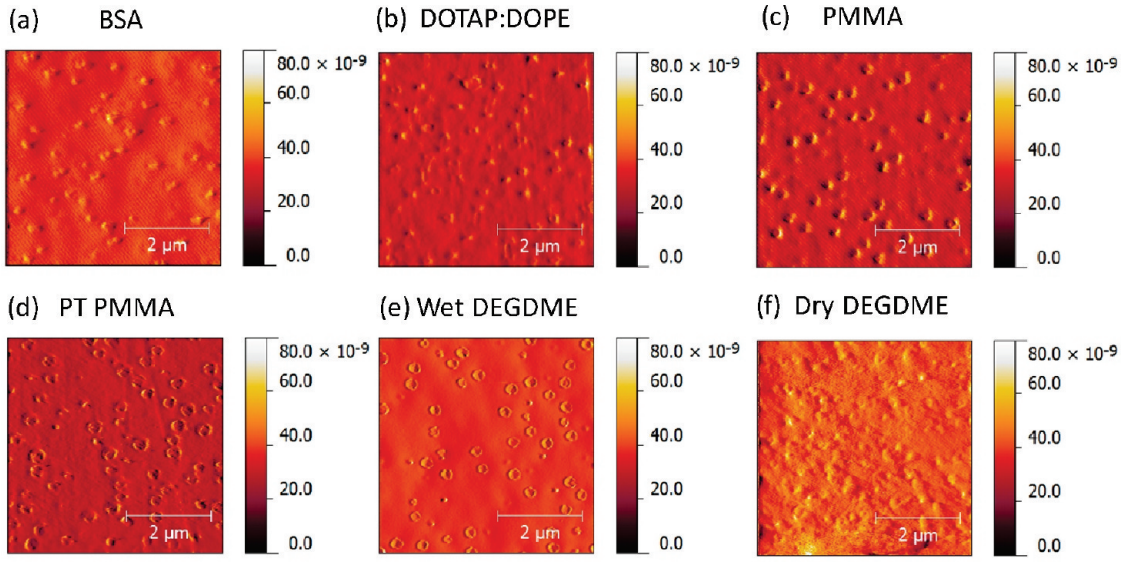

Figure 4. AFM images in contact mode of PMMA sheets deposited with different blocking agents: (a) BSA (rms = 9.62 ± 2.58 nm), (b) DOTAP:DOPE (rms = 4.49 ± 0.09 nm), (e) wet DEGDME (rms = 16.63 ± 3.17 nm), and (f) dry DEGDME (rms = 21.1 ± 9.46 nm). For comparison, the AFM image of plain and PT PMMA surface are also shown in (c) (rms = 4.06 ± 0.50 nm) and (d) (rms = 3.56 ± 0.62 nm), respectively. The AFM surface topologies together with the WCA data in Figure 3 clearly confirm the successful coatings of BSA, DOTAP:DOPE, and wet and dry DEGDME onto the PMMA surface.

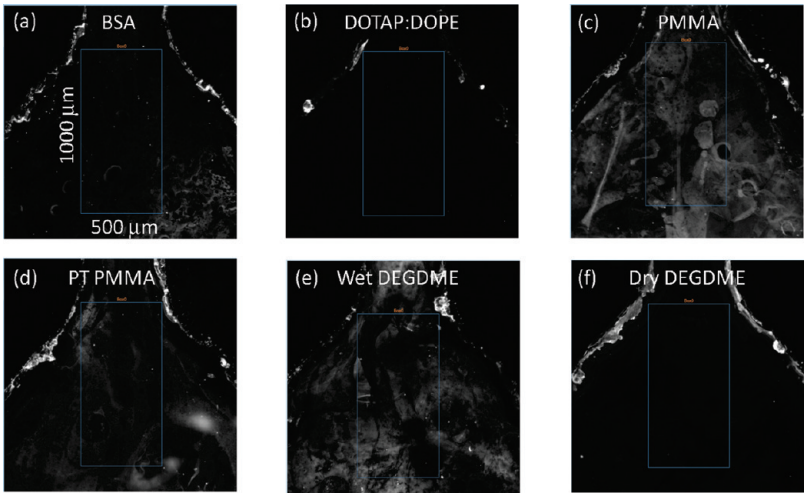

Figure 5. Fluorescent images on the reaction chambers of the flow-cell deposited with Cy5-anti-IgG (25 μg/mL) after 60 min of reaction on (a) BSA, (b) DOTAP:DOPE, (e) wet DEGDME, and (f) dry DEGDME coatings, respectively. For comparison, the fluorescent images of the same regions on the plain and PT PMMA flow-cell are shown in panels c and d, respectively. As can be seen, the DOTAP:DOPE and dry DEGDME not only suppressed the nonspecific binding of Cy5-anti-IgG effectively but also uniformly across the reaction chambers. On the other hand, the Cy5-anti-IgG bound very randomly to the plain PMMA and wet DEGDME coatings, resulting in highly nonuniform fluorescent intensity across the reaction chambers.

We therefore believe that it is not the roughness but the vast hydration that is the dominant factor responsible for its increased protein repellent properties.

3.2. Blocking Effects Measured by Fluorescence Microscopy. The fluorescent images of the reaction wells of the modified PMMA flow-cell deposited with Cy5-labeled anti-IgG are shown in Figure 5a—f. The rectangular areas of 500 μm × 1000 μm in the expanded regions of the PMMA microwells were used to measure the mean and the standard deviation of fluorescent intensities. The Cy5-labeled anti-IgG adsorbed on plain PMMA microwell surfaces showed very uneven fluorescent intensity. It could be speculated that the protein anti-IgG's were absorbed randomly depending on their preferences toward the hydrophobic PMMA surface. Of all the blocking agents tested, DOTAP:DOPE resulted in the most uniform and effective blocking as shown in Figure 5b. The BSA and dry DEGDME also resulted in a relatively good and uniform blocking. The fluorescent intensity measurements inside the rectangular areas shown in Figure 6 confirmed the observation from fluorescent images in Figure 5. The fluorescent intensity of the absorbed Cy5-labeled anti-IgG onto the DOTAP:DOPE-coated PMMA microwell showed the smallest value. On the other hand, without any blocking agent, the fluorescent intensity was the highest and very nonuniform. The blocking due to dry DEGDME coating

dx.doi.org/10.1021/la2011502 |*Langmuir* 2011, 27, 9043–9051

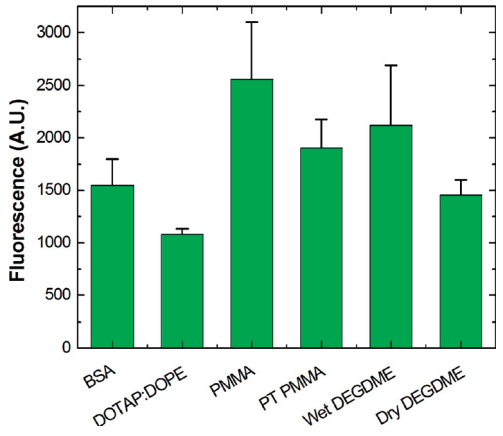

Figure 6. Fluorescent intensities measured on the rectangular areas indicated in Figure 5 of PMMA flow-cells deposited with 30 μL of Cy5-labeled anti-IgG with concentrations of 25 μg/mL in PBS (pH 7.4). The error bars represent the standard deviations of the fluorescent intensities of the pixels inside the rectangular areas. This result again confirms the superiority of DOTAP:DOPE and dry DEGDME coatings compared to the remaining coatings for blocking Cy5-labeled anti-IgG nonspecific binding onto the PMMA surface.

was as good as that due to BSA. BSA, with concentration typically ranging from 0.5 − 3% w/w, is widely used for blocking the nonspecific adsorption of proteins.[29] Interestingly, the cationic DOTAP:DOPE showed very good blocking with respect to protein nonspecific adsorption. The blocking effect of DOTAP has been shown previously inside fused silica capillary.[30] Here is the first time it has been shown to significantly reduce the nonspecific adsorption of proteins onto PMMA surface. Both the BSA and the DOTAP:DOPE films represent examples where the predominant forces responsible for the low protein adsorption are based on electrostatic interactions. Such repulsive (or attractive) forces can be relatively easily tuned to repel specific proteins by adjusting the pH of the solution above (or below, depending on the charge of the modified PMMA surface) the isoelectric point of the given protein. The repulsion of proteins by PEG-like materials from DEGDME is also in agreement with previous work.[32] It is also interesting to note that the dry DEGDME prepared by PECVD showed superior blocking performance compared to that of wet DEGDME. Moreover, the blocking due to wet DEGDME was not uniform inside the microwell. It could be due to the fact that in the wet preparation of a DEGDME film, the DEGDME molecules were simply adsorbed onto the activated PMMA surface while for the dry plasma deposition of a DEGDME film, an intermediate TEOS layer was inserted and formed a robust scaffold for the DEGDME to be built on, while the plasma promoted reaction and cross-linking of the layer. The PT PMMA surface showed relatively uniform adsorption of proteins in contrast to the plain PMMA surface. It has been shown previously that oxygen plasma treatment creates carboxylic groups and other reactive radicals on the PMMA surface which could allow the binding of the proteins.[35]

3.3. Stability of Blocking Agents and Their Effects on Subsequent Anti-α-hCG Adsorption Assay. The Ψ and Δ spectra measured on the Au-coated surface after rinsing the blocking agent-coated PMMA flow-cells with PBS buffer for 15 min, followed by adsorption of anti-α-hCG for 60 min are shown in Figure 7a−e. Since it is not possible to perform TIRE measurements without the presence of aqueous buffer inside the microwells, the first set of Ψ and Δ spectra reflected not only the Au film but also any materials that could be removed from the PMMA flow-cell and deposited onto the Au surface after rinsing with PBS for 15 min.[17] The SPR wavelength of the first set of spectra varied from well to well, which was understandable since the optical alignment and the thickness of the organic materials deposited from the PBS rinsing might be different. Nevertheless, the SPR wavelength was centered around 700 nm. After the first set of Ψ and Δ spectra, the second set of Ψ and Δ spectra corresponding to the adsorption of 50 μg/mL of anti-α-hCG to the contaminated Au sensing surface showed different shifts from microwell to microwell. For the DOTAP:DOPE and BSA-coated microwells, the relative shifts were very small from the first Ψ and Δ spectra. We reasoned that some of the DOTAP:DOPE and BSA might have been removed from the PMMA flow-cell and deposited back onto the Au surface, thus blocking the subsequent binding of the anti-α-hCG. Accordingly, this resulted in only a very small shift in the Ψ and Δ spectra. For the remaining plain, PT, wet, and dry DEGDME-coated microwells, the shifts were very distinctive and large, meaning a large amount of anti-α-hCG had been deposited onto the Au sensing surface.

Fitting results of the first Ψ and Δ spectra to a four-layer model gave the thickness of organic materials being deposited onto the Au surface after rinsing with PBS after 15 min (Figure 8). The results indicate that BSA and DOTAP:DOPE had been desorbed from BSA and DOTAP:DOPE-coated microwells, respectively, and were then deposited back on the sensing Au surface. Despite the fact that the DOTAP:DOPE film deposited onto a PMMA surface has been shown to have very good protein blocking performance, this cationic lipid appears to not be very stable in aqueous environment, as has also been shown in the case of DODAB film.[36] It seems that the cumulative effect of the van der Waals forces between the hydrophobic chain of DOTAP:DOPE and the methoxy groups of PMMA is not strong enough to maintain their adhesion under aqueous conditions. Similarly, the BSA film was also formed by physical adsorption of BSA onto the PMMA microwells, thus some loosely bound BSA might have also been removed due to the rinsing with PBS. The dimensions of BSA are $14 \times 4 \times 4$ nm^3. The DOTAP molecule is composed of the hydrophobic part of the lipid, which is ~2.1 nm in size, and the hydrophilic part, which is another ~1 nm in size, while the DOPE molecule has a size of 2.9 nm.[37] Furthermore, it has also been shown that a mixed DOTAP:DOPE film formed on a mica surface has a thickness ranging from 2.4 to 2.9 nm.[38] From the ellipsometric fitting in Figure 8 and the size of BSA and DOTAP or DOPE molecules, it is likely that a monolayer of BSA (lying flat) and DOTAP:DOPE have been readsorbed onto the Au surface. It is interesting to note that the wet DEGDME also showed a relatively large thickness of organic layer deposited. This could be explained by the fact that the DEGDME has only been dynamically coated onto the PT PMMA surface, thus some loosely bound DEGDME might have been removed and deposited back to the Au surface. The plain, PT PMMA, and dry DEGDME-coated microwells showed a very thin layer of organic materials deposited onto the Au surface, confirming their stability and resistance against washing in buffered solution. The small amount of deposited organic material could come from contaminants of the PBS buffer being used. Overall, the dry DEGDME film, covalently cross-linked with siloxane (TEOS), is very robust compared to other coatings under the rinsing effect of PBS flow inside the microwell.

The increases in the thickness after adsorption of anti-α-hCG onto the Au sensing substrate are shown in Figure 9. We

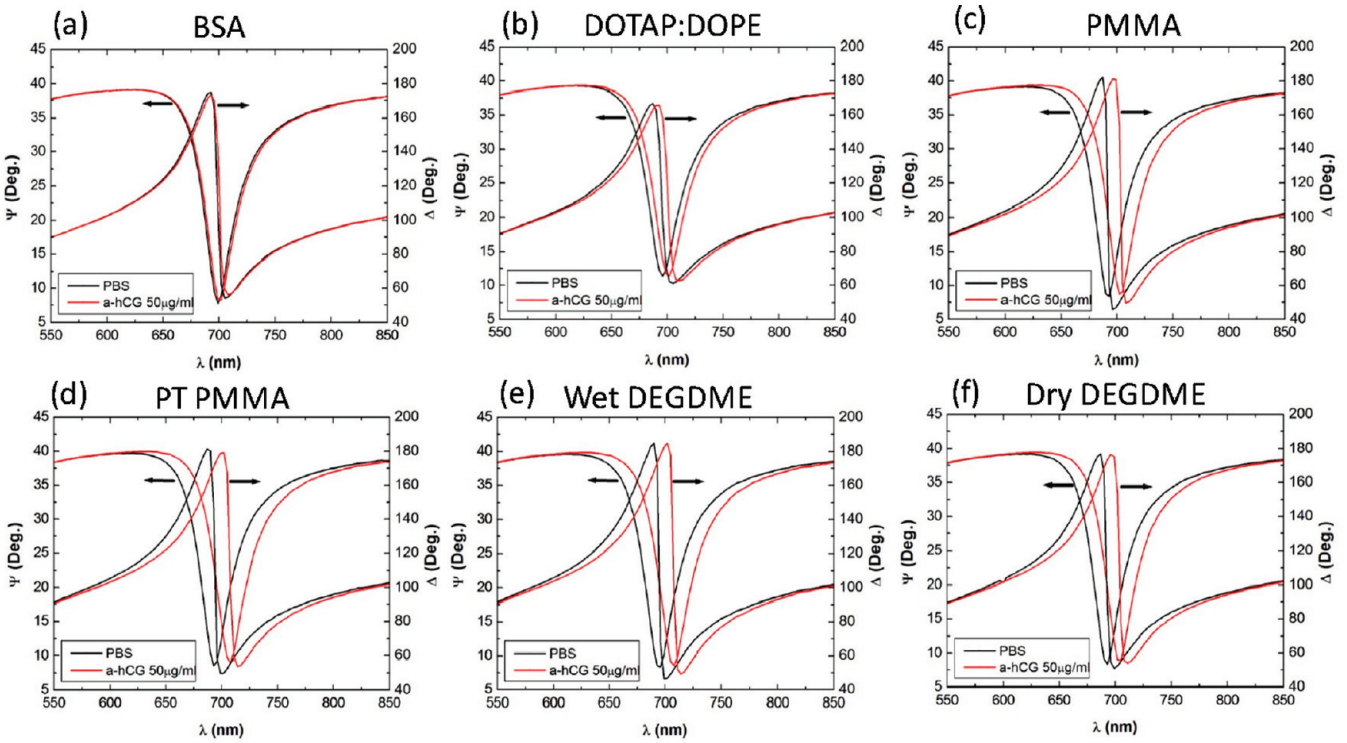

Figure 7. Ψ and Δ spectral shifts after adsorption of anti-α-hCG 50 μg/mL over 60 min onto Au-coated glass sensing substrate in PMMA microwells blocked with (a) BSA, (b) DOTAP:DOPE, (e) wet DEGDME, and (f) dry DEGDME. For comparison, the spectral shifts in plain and PT PMMA microwells are also shown in panels c and d, respectively. Note that the PBS spectra in all panels do not represent PBS buffer on plain gold surfaces, but they represent PBS buffer on contaminated gold surfaces deposited with any organic materials removed by rinsing the coatings with PBS buffer for 15 min at 5 μL/min.

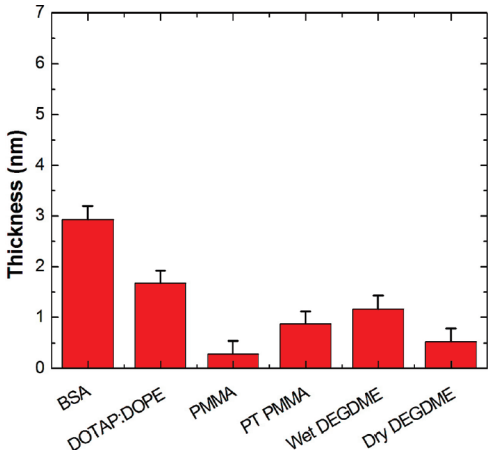

Figure 8. Thickness of organic layer removed from the coating materials and deposited back onto the Au surface after rinsing the microwells with PBS buffer for 15 min at a flow rate of 5 μL/min. A four-layer ellipsometric model was used in the fitting with the PsiDelta 2 software (Jobin Yvon Horiba, France) to estimate the thickness of the organic layer. A Cauchy dispersion formula $A + B/\lambda^2 + C/\lambda^4$, where A = 1.415, B = 0.01 nm^2, and C = 0 was used to model the refractive indices of all organic layers with the assumption that the difference in their refractive indices is negligible.[21] In this case, the larger the thicknesses (e.g., BSA and DOTAP:DOPE), the less stable the corresponding coatings against buffer washing.

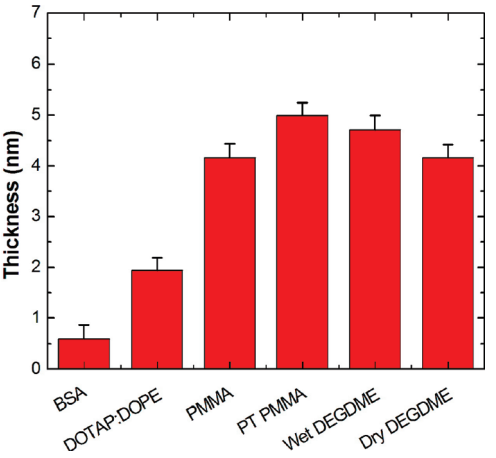

Figure 9. Thicknesses of anti-α-hCG at 50 μg/mL deposited onto contaminated Au surfaces in different microwells after 60 min of reaction. Here, contaminated Au surfaces are Au surfaces deposited with organic layers removed from the coatings. These thicknesses of anti-α-hCG were obtained by subtracting the absolute thicknesses from the ellipsometric fitting to the thicknesses of the organic layers in Figure 8.[21] In this case, anti-α-hCG physisorbed much less to the Au surfaces contaminated with BSA and DOTAP:DOPE removed from the coatings.

observed a small thickness increment after adsorption of anti-α-hCG onto the contaminated Au sensing surface inside the DOTAP:DOPE and BSA-coated microwells, whereas the remaining four microwells including plain, PT, wet, and dry DEGDME showed good adsorption of the protein onto the Au surface, as evidenced by large thickness increments. Finally, the kinetic data of

dx.doi.org/10.1021/la2011502 |*Langmuir* 2011, 27, 9043–9051

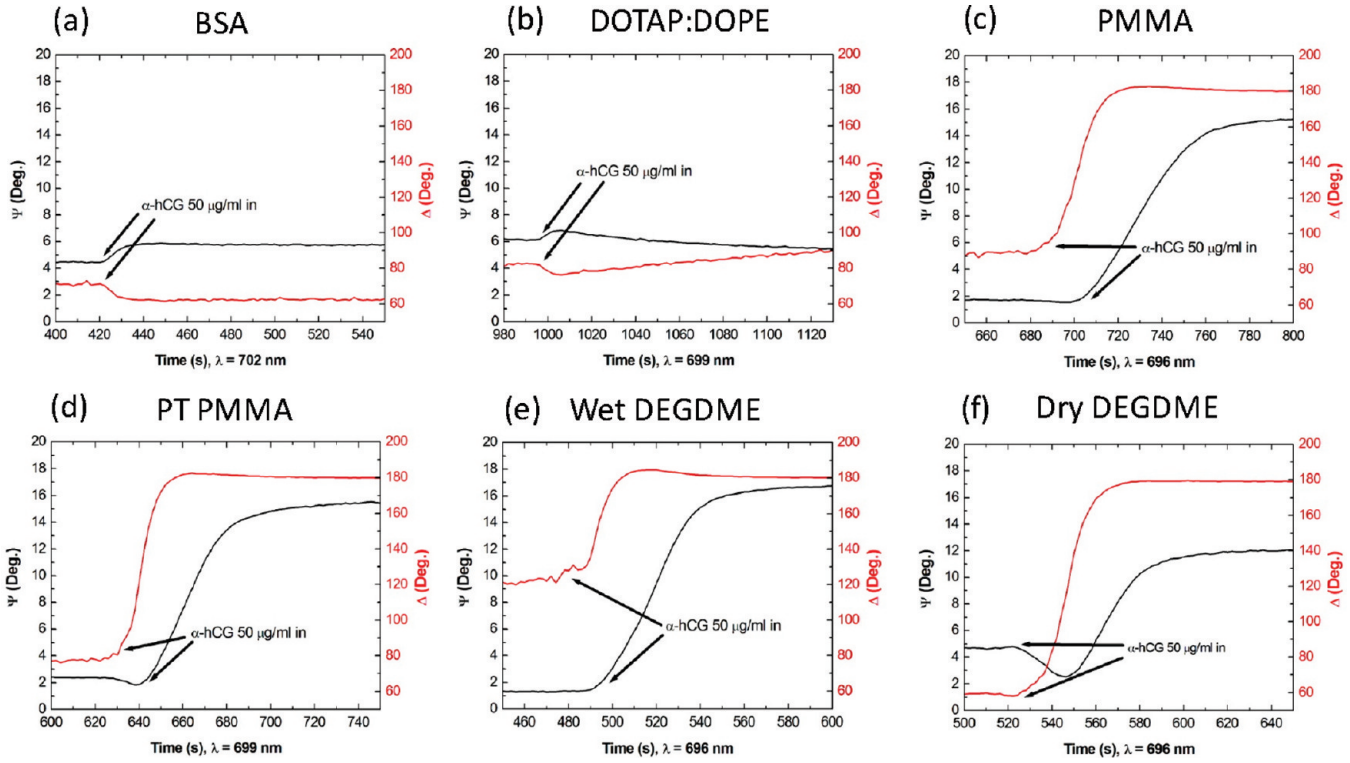

Figure 10. Kinetics of Ψ and Δ measured on the Au substrates before and after injection of anti-α-hCG at 50 μg/mL in different PMMA microwells blocked with (a) BSA, (b) DOTAP:DOPE, (e) wet DEGDME, and (f) dry DEGDME. For comparison, the kinetics of Ψ and Δ in plain and PT PMMA microwells were also shown in panels c and d, respectively. For DOTAP:DOPE and BSA coatings, the Au surfaces have been blocked by a layer of DOTAP:DOPE and BSA removed from the PMMA surfaces of the microwells, thus preventing the physisorption of anti-α-hCG (i.e., the rates change of Ψ and Δ are very slow compared to other coatings). The flow-rate of the syringe pump was adjusted at 5 μL/min. The kinetic wavelength was chosen to maximize the change in Ψ and Δ signal.

the change in Ψ and Δ from the PBS rinsing to the introduction of α-anti-hCG convincingly showed the effect of contamination of the Au surface by desorbed blocking agents (Figure 10). In BSA and DOTAP:DOPE-coated microwells, the Ψ and Δ responses were very slow, implying that the Au surface of the sensing substrate has been contaminated and partially blocked, thus reducing the rate of adsorption of the proteins. On the other hand, the adsorption happened very fast, i.e. within 30 to 40 s, on the PMMA microwells blocked by wet and dry DEGDME as well as in the plain and PT PMMA microwells. This strongly supports our hypothesis about the effect of the desorption of blocking agents with respect to the subsequent assays which are based-on the adsorption of anti-α-hCG onto the Au sensing substrates. We expect this finding would be useful in the assessment of nonspecific adsorption blocking agents for PMMA-based immunosensor or biosensor devices.[22−26]

4. CONCLUSIONS

A comprehensive comparison of different surface coatings for suppression of nonspecific adsorption on PMMA surfaces has been carried out. Measurements using WCA and AFM confirmed the successful modification of the PMMA surfaces with blocking agents. Fluorescent measurements show that the DOTAP:DOPE is the best of all the coatings tested to suppress the nonspecific binding of Cy5-labeled anti-IgG onto the PMMA surface. BSA and plasma-deposited dry DEGDME coatings also showed very good suppression of nonspecific adsorption of proteins. However, results obtained from TIRE showed that DOTAP:DOPE and BSA could be removed from PMMA surfaces upon rinsing with PBS buffer and deposited back onto Au sensing substrate. The contamination of the Au sensing substrate by desorbed blocking agents was manifested in the kinetics and the amounts of the adsorbed anti-α-hCG proteins. Overall, the dry DEGDME coating deposited by PECVD showed very good blocking and excellent stability when rinsing with PBS buffer. Our results could be useful when one considers blocking agents to suppress the nonspecific adsorption of analyte inside PMMA devices. In particular, it would have implications on PMMA-based biosensor devices integrated with sensing elements for electrochemical or optical detection.

AUTHOR INFORMATION

Corresponding Author

*E-mail: nam.le@csiro.au.

Present Addresses

[||]CSIRO Materials Science and Engineering, Highett, Victoria 3190, Australia.

ACKNOWLEDGMENT

This material is based upon work supported by the Science Foundation Ireland under Grant No. SFI/10/CE/B1821. D.E.W. is an ETS Walton Visiting Fellow of the Science Foundation Ireland.

REFERENCES

(1) Reyes, D. R.; Iossifidis, D.; Auroux, P.-A.; Manz, A. Micro total analysis systems. 1. Introduction, theory, and technology. *Anal. Chem.* **2002**, *74*, 2623–2636.

(2) Auroux, P.-A.; Iossifidis, D.; Reyes, D. R.; Manz, A. Micro total analysis systems. 2. Analytical standard operations and applications. *Anal. Chem.* **2002**, *74*, 2637–2652.

(3) Dittrich, P. S.; Tachikawa, K.; Manz, A. Micro total analysis systems. Latest advancements and trends. *Anal. Chem.* **2006**, *78*, 3887–3908.

(4) West, J.; Becker, M.; Tombrink, S.; Manz, A. Micro total analysis systems: Latest achievements. *Anal. Chem.* **2008**, *80*, 4403–4419.

(5) Marie, R.; Beech, J. P.; Voros, J.; Tegenfeldt, J. O.; Hook, F. Use of PLL-*g*-PEG in micro-fluidic devices for localizing selective and specific protein binding. *Langmuir* **2006**, *22*, 10103–10108.

(6) Liu, J.; Lee, M. L. Permanent surface modification of polymeric capillary electrophoresis microchips for protein and peptide analysis. *Electrophoresis* **2006**, *27*, 3533–3546.

(7) Bi, H.; Meng, S.; Li, Y.; Guo, K.; Chen, Y.; Kong, J.; Yang, P.; Zhong, W.; Liu, B. Deposition of PEG onto PMMA microchannel surface to minimize nonspecific adsorption. *Lab Chip* **2006**, *6*, 769–775.

(8) Muck, A.; Svatoš, A. Chemical modification of polymeric microchip devices. *Talanta* **2007**, *74*, 333–341.

(9) Lin, Y. W.; Chang, H. T. Modification of poly(methyl methacrylate) microchannels for highly efficient and reproducible electrophoretic separations of double-stranded DNA. *J. Chromatogr. A* **2005**, *1073*, 191–199.

(10) Dang, F.; Kakehi, K.; Cheng, J.; Tabata, O.; Kurokawa, M.; Nakajima, K.; Ishikawa, M.; Baba, Y. Hybrid dynamic coating with *n*-dodecyl *β*-D-maltoside and methyl cellulose for high-performance carbohydrate analysis on poly(methyl methacrylate) chips. *Anal. Chem.* **2006**, *78*, 1452–1458.

(11) Mohamadi, M. R.; Mahmoudian, L.; Kaji, N.; Tokeshi, N.; Baba, Y. Dynamic coating using methylcellulose and polysorbate 20 for nondenaturing electrophoresis of proteins on plastic microchips. *Electrophoresis* **2007**, *28*, 830–836.

(12) Lai, S.; Cao, X.; Lee, L. J. A packaging technique for polymer microfluidic platforms. *Anal. Chem.* **2004**, *76*, 1175–1183.

(13) Liu, J.; Pan, T.; Woolley, A. T.; Lee, M. L. Surface-modified poly(methyl methacrylate) capillary electrophoresis microchips for protein and peptide analysis. *Anal. Chem.* **2004**, *76*, 6948–6955.

(14) Westphal, P; Bornmann, A Biomolecular detection by surface plasmon enhanced ellipsometry. *Sens. Actuators, B* **2002**, *84*, 278–282.

(15) Arwin, H.; Poksinski, M.; Johansen, K. Total internal reflection ellipsometry: Principles and applications. *Appl. Opt.* **2004**, *43*, 3028–3036.

(16) Poksinski, M.; Arwin, H. Protein monolayers monitored by internal reflection ellipsometry. *Thin Solid Films* **2004**, *455−456C*, 716–721.

(17) Poksinski, M.; Arwin, H. Total internal reflection ellipsometry: Ultrahigh sensitivity for protein adsorption on metal surfaces. *Opt. Lett.* **2007**, *32*, 1308–1310.

(18) Nabok, A.; Tsargorodskaya, A.; Hassan, A. K.; Starodub, N. F. Total internal reflection ellipsometry and SPR detection of low molecular weight environmental toxins. *Appl. Surf. Sci.* **2005**, *246*, 381–386.

(19) Nabok, A.; Tsargorodskaya, A.; Davis, F.; Higson, S. P. J. The study of genomic DNA adsorption and subsequent interactions using total internal reflection ellipsometry. *Biosens. Bioelectron.* **2007**, *23*, 377–383.

(20) Nabok, A; Tsargorodskaya, A.; Holloway, A; Starodub, N. F.; Demchenko, A. Specific binding of large aggregates of amphiphilic molecules to the respective antibodies. *Langmuir* **2007**, *23*, 8485–8490.

(21) Le, N. C. H.; Gubala, V.; Gandhiraman, P. R.; Coyle, C.; Daniels, S.; Williams, D. E. Total internal reflection ellipsometry (TIRE) as a label-free assessment method for optimization of the reactive surface of bioassay devices based on a functionalized cyclo olefin polymer. *Anal. Bioanal. Chem.* **2010**, *398*, 1927–1936.

(22) Qi, S.; Liu, X.; Ford, S.; Barrows, J.; Thomas, G.; Kelly, K; McCandless, A; Lian, K.; Goettert, J.; Soper, S. A. Microfluidic devices fabricated in poly(methyl methacrylate) using hot-embossing with integrated sampling capillary and fiber optics for fluorescence detection. *Lab Chip* **2002**, *2*, 88–95.

(23) Horng, R. H.; Han, P.; Chen, H. Y.; Lin, K. W.; Tsai, T. M.; Zen, J. M. PMMA-based capillary electrophoresis electrochemical detection microchip fabrication. *J. Micromech. Microeng.* **2005**, *15*, 6–10.

(24) Bai, Y.; Koh, C. G.; Boreman, M.; Juang, Y.; Tang, I.; Lee, L. J.; Yang, S. Surface modification for enhancing antibody binding on polymer-based microfluidic device for enzyme-linked immunosorbent assay. *Langmuir* **2006**, *22*, 9458–9467.

(25) Nugen, S. R.; Asiello, P. J.; Connelly, J. T.; Baeumner, A. J. PMMA biosensor for nucleic acids with integrated mixer and electrochemical detection. *Biosens. Bioelectron.* **2009**, *24*, 2428–2433.

(26) Baldini, F.; Carloni, A.; Giannetti, A.; Porro, G.; Trono, C. An optical PMMA biochip based on fluorescence anisotropy: Application to C-reactive protein assay. *Sens. Actuators, B* **2009**, *139*, 64–68.

(27) Hamada, K.; Yamashita, K.; Serizawa, T.; Kitayama, T.; Akashi, M. Adsorption of bovine serum albumin onto poly(methyl methacrylate) stereocomplex films with a molecularly regulated nanostructure. *J. Polym. Sci., Part A: Polym. Chem.* **2003**, *41*, 1807–1812.

(28) Tsougeni, K.; Petrou, P. S.; Tserepi, A.; Kakabakos, S. E.; Gogolides, E. Nano-texturing of poly(methyl methacrylate) polymer using plasma processes and applications in wetting control and protein adsorption. *Microelectron. Eng.* **2009**, *86*, 1424–1427.

(29) Jensen, J.; Hoiby, P.; Emiliyanov, G.; Bang, O.; Pedersen, L.; Bjarklev, A. Selective detection of antibodies in microstructured polymer optical fibers. *Opt. Express* **2005**, *13*, 5883–5889.

(30) Bonoli, M.; Varjo, S. J.O.; Wiedmer, S. K.; Riekkola, M.-L. Cationic lipid vesicles as coating precursors in capillary electrochromatography: Separation of basic proteins and neutral steroids. *J. Chromatogr. A* **2006**, *1119*, 163–169.

(31) Sardella, E.; Gristina, R.; Senesi, G. S.; d'Agostino, R; Favia, R. Homogeneous and micro-patterned plasma-deposited PEO-like coatings for biomedical surfaces. *Plasma Process. Polym.* **2004**, *1*, 63–72.

(32) Valsesia, A.; Colpo, A.; Meziani, T.; Bretagnol, F.; Lejeune, M.; Rossi, F.; Bouma, A.; Garcia-Parajo, M. Selective immobilization of protein clusters on polymeric nanocraters. *Adv. Funct. Mater.* **2006**, *16*, 1242–1246.

(33) Belegrinou, S.; Mannelli, I.; Lisboa, P.; Bretagnol, F.; Valsesia, A.; Ceccone, G.; Colpo, P.; Rauscher, H.; Rossi, F. pH-Dependent immobilization of proteins on surfaces functionalized by plasma-enhanced chemical vapor deposition of poly(acrylic acid)- and poly(ethylene oxide)-like films. *Langmuir* **2008**, *24*, 7251–7261.

(34) Gandhiraman, R. P.; Karkari, S. K.; Daniels, S. M.; MacCraith, B. D. Influence of ion bombardment on the surface functionalization of plasma deposited coatings. *Surf. Coat. Technol.* **2009**, *203*, 3521–3526.

(35) Brown, L.; Koerner, T.; Horton, J. H.; Oleschuk, R. D. Fabrication and characterization of poly(methylmethacrylate) microfluidic devices bonded using surface modifications and solvents. *Lab Chip* **2006**, *6*, 66–73.

(36) Pereira, E. M. A.; Kosaka, P. M.; Rosa, H.; Vieira, D. B.; Kawano, Y.; Petri, D. F. S.; Carmona-Ribeiro, A. M. Hybrid materials from intermolecular associations between cationic lipid and polymers. *J. Phys. Chem. B* **2008**, *112*, 9301–9310.

(37) Dufrene, Y. F.; Barger, W. R.; Green, J.-B. D.; Lee, G. U. Nanometer-scale surface properties of mixed phospholipid monolayers and bilayers. *Langmuir* **1997**, *13*, 4779–4784.

(38) Leonenko, Z. V.; Merkle, D.; Lees-Miller, S. P.; Cramb, D. T. Lipid phase dependence of DNA−cationic phospholipid bilayer interactions examined using atomic force microscopy. *Langmuir* **2002**, *18*, 4873–4884.